High frequency poroelastic waves in hydrogels

Piero Chiarelli
CNR Institute of Clinical Physiology, via Moruzzi 1, 56124 Pisa, Italy

Antonio Lanatà and Marina Carbone
Interdepartmental Research Center "E. Piaggio," Faculty of Engineering, University of Pisa, via Diotisalvi 2, 56126 Pisa, Italy

Claudio Domenici
CNR Institute of Clinical Physiology, via Moruzzi 1, 56124 Pisa, Italy

(Received 3 December 2008; revised 25 September 2009; accepted 22 December 2009)

In this work a continuum model for high frequency poroelastic longitudinal waves in hydrogels is presented. A viscoelastic force describing the interaction between the polymer network and the bounded water present in such materials is introduced. The model is tested by means of ultrasound wave speed and attenuation measurements in polyvinylalcohol hydrogel samples. The theory and experiments show that ultrasound attenuation decreases linearly with the increase in the water volume fraction β of the hydrogel. The introduction of the viscoelastic force between the bounded water and the polymer network leads to a bi-phasic theory, showing an ultrasonic fast wave attenuation that can vary as a function of the frequency with a non-integer exponent in agreement with the experimental data in literature. When β tends to 1 (100% of interstitial water) due to the presence of bounded water in the hydrogel, the ultrasound phase velocity acquires higher value than that of pure water. The ultrasound speed gap at $\beta=1$ is confirmed by the experimental results, showing that it increases in less cross-linked gel samples which own a higher concentration of bounded water. © *2010 Acoustical Society of America.* [DOI: 10.1121/1.3293000]

PACS number(s): 43.20.Jr, 43.20.Bi, 43.80.Cs, 43.80.Ev [ADP] Pages: 1197–1207

I. INTRODUCTION

The present work is motivated in defining a reliable model for ultrasound (US) wave propagation both in hydrogels[1–5] and in extra-cellular matrices of natural soft tissues.[6–8]

In fact, even if the structure of a synthetic hydrogel is somehow different from that one of extra-cellular matrices with proteoglycans exists a strong analogy between the macroscopic response of charged hydrogels and that one of natural matrices, such as that one of derma,[9] in the diffusional wave limit.

On this basis, the US model for hydrogels can be a theoretical tool for the study and the characterization of tissue-mimicking phantom for US thermal therapy and for the development of non-invasive assessment method of soft tissue stiffness.[10–12]

This possibility is confirmed by the current research investigations that clearly show how the knowledge of the link between the poroelastic characteristics of a biological tissue and its acoustical behavior is a source of information that can be used for non-invasive investigation techniques.[13,14]

On the other hand, the US propagation in natural hydrogels, mostly composed of water, is usually modeled by means of the wave equation that holds for liquids.[5] Even if this approach is sufficiently satisfying, it does not completely explain the experimental behavior of US.

There are many discrepancies between US propagation in water and in natural hydrogels of soft tissues both for transverse and longitudinal acoustic waves.[6–8]

As far as longitudinal waves in biological gels are concerned, in the US absorption frequency law $\nu^{(1+\delta)}$ (where ν is the US frequency) δ ranges between $\frac{1}{4}$ and $\frac{1}{2}$, while it holds that $\delta=1$ for water.[15]

The fractional value of δ cannot also be explained by means of the established bi-phasic theories that lead to a frequency dependence equal to that of water with $\delta=1$.[16,17]

The bi-phasic models of the acoustic wave propagation were born in geology and engineering sciences[18–22] from where they received a clear imprinting. All proposed theories[16–24] do not abandon the scheme of a solid matrix permeated by a well distinguishable fluid.

Actually, it is quite evident that gels constitute a possible exception where the solid phase and the liquid one are chemically interacting and the boundary is not simply defined. As a matter of fact, the presence of the bounded water around the polymer chains creates a bearing whose thickness and viscous force do not follow the fluid dynamics laws.[19,20]

In order to solve this theoretical leak, in the present paper, a viscoelastic matrix-fluid interaction specific for hydrogels is introduced.

The hydrogel structure is somewhere between a solid and a liquid. It consists of polymers, or long chain molecules, which are cross-linked to create an entangled network immersed in a liquid medium that fills the intra-molecular interstices.

The properties of gels are strongly influenced by the interaction of these two components.

First, gels were conceptualized as porous media consisting of two interpenetrating macroscopic substances (an elas-

tic and porous solid matrix and a fluid). An elegant and satisfying theory based on this approach is the poroelastic model developed by Biot.[16,17,23,24]

One of the main characteristics of the Biot theory is that the dissipative relaxation is mainly ascribed to the relative motion of fluid against solid, while dissipations within fluid and solid are neglected.

At low frequencies, the friction of the fluid that moves against the solid network leads to a "diffusional" wave, giving theoretical forecasts that well agree with many experimental results.[9,25–29] Instead, this solid-fluid interaction scheme becomes inadequate at high frequencies.

In order to obtain a more satisfying model to describe how ultrasounds propagate in hydrogels, we propose a new mechanism of interaction between the fluid (water) and the solid matrix (polymer network).

The main mathematical statement, introduced here, takes into account the presence of the bounded water attached to the polymeric network of the hydrogel. The fluid-matrix interaction is modeled by ascribing a viscoelastic force between the polymer matrix and the bounded water around it, while a viscous force between the "polymer-bounded water aggregate" and the interstitial free water is assumed.

This assumption leads to relevant outcomes concerning the US propagation in gels. As confirmed by the experiments, the effect of the bounded water in hydrogels on the US speed is quite relevant as well as the frequency dependence of their attenuation. The model of the US propagation in hydrogels can lead to the understanding of their behavior and how it takes origin from the poroelastic structure. The possibility to describe the US propagation in terms of the poroelastic characteristics of both cells and extra-cellular matrix may lead to US non-invasive technique for the evaluation of the tissue physiology since the permeability and elasticity of the cell structures are directly related to their state and functionality.

In the following we derive the phase velocity of longitudinal US plane waves and their attenuation in hydrogels (Sec. II) by using the proposed fluid-matrix interaction.

Then, in Sec. III, we compare the theoretical forecasts with the outcomes of experimental measurements.

II. POROELASTIC WAVES IN HYDROGELS

Biot's[16,17] theory is carried out by assuming that the fluid motion in the pores follows the Poiseuille flow. In this case, the characteristic boundary, where the velocity attains a certain percentage of its maximum, is known as the viscous skin depth[19,20] $(\eta_d/\pi\nu\rho_f)^{1/2}$, where ρ_f and η_d are the fluid mass density and its dynamic viscosity, respectively. In the low frequency limit, this layer becomes larger than the pore diameter and the velocity profile can be assumed parabolic. At higher frequencies, when the viscous skin depth is smaller than the pore size, Biot[17] added a compensating factor $F_{(\nu)}$ to the fluid-solid friction coefficient f to take into account for the divergence by the Poiseuille flow. He stated that $F_{(\nu)}$ increases according to the law $\lim_{\nu/\nu c\to\infty} F_{(\nu)} \propto (\nu/\nu_c)^{1/2}$, where $\nu_c = f/\rho_f$ and f is the zero frequency friction coefficient[23] (i.e., the inverse of the hydraulic permeability of the medium).

Given that pore dimensions are very small in gels, the crossover frequency ν_c is very high [for instance, polyvinylalcohol (PVA)-polyacrylic acid hydrogels[30] show $\nu_c \approx 10^{13}$ Hz, close to the maximum frequency allowed in material media]. Therefore, for usual US frequencies the factor $F_{(\nu)}$ in hydrogels should be always used in the low frequency limit (i.e., $F_{(\nu)}=1$). This fact gives the US attenuation[17] proportional to ν^2 while the experimental results follow the law[15] $\propto \nu^n$ with n ranging between 1,25 and 1,50.

In the frame of the bi-phasic approach one possible way out is to consider a different fluid-network interaction for hydrogels.

If we look at the hydrogel structure, it shows water molecules that are bounded to the matrix polymer chains by means of chemical interactions. The local polymer field organizes the water molecules around itself in a way that they can be assumed radially bounded to its chains, while relatively free to move along the perpendicular direction in a viscous manner. Due to the fact that in an isotropic gel the polymer chains are oriented in all directions, under the elastic wave action, the bounded water molecules will respond in an elastic and viscous manner as a mean. Thence, a more appropriate matrix-fluid interaction scheme is assumed:

(i) a viscoelastic interaction between the bounded water and the polymer matrix (with an elastic constant k and a friction coefficient η) and
(ii) a pure viscous interaction between the bounded water molecules (surrounding the polymer network) and the free water.

A. Compressional waves for dilute poroelastic media

Since the percentile content of water in gels is often very high (up to 99%), in the low frequency limit the poroelastic theories for hydrogels make historically use of the dilute matrix approximation[30–33] [i.e., $\beta \approx 1$, where $\beta = V_w/(V_w + V_p)$, where V_w and V_p are the volumes of water and polymer, respectively]. Such an approximation works very well even for gels with a remarkable polymer content (owing β down to 0.50).

For the high frequency limit, the dilute matrix approximation does not work so well especially for the US wave speed that shows to be sensibly dependent on the polymer content for values of β up to 0.7. Nevertheless, the dilute matrix approximation is still physically meaningful for β bigger than 0.8 where it clearly defines the behavior of the US wave speed.

Before introducing the specific hydrogel fluid-matrix interaction, we derive the poroelastic longitudinal wave equations in the limit of very dilute matrix with incompressible solid and liquid constituents.

In this case the compressional elastic moduli of the fluid and the solid matrix can be assumed to be greater than all the other elastic moduli in the poroelastic longitudinal wave equations[16,17,23,24] that read

$$\nabla^2(P\varepsilon_{\alpha\alpha}+Qe_{\alpha\alpha})=\partial^2(\rho_{11}\varepsilon_{\alpha\alpha}+\rho_{12}e_{\alpha\alpha})/\partial t^2 + \beta f F_{(\nu)}\,\partial(\varepsilon_{\alpha\alpha}-e_{\alpha\alpha})/\partial t, \quad (1)$$

$$\nabla^2(Q\varepsilon_{\alpha\alpha}+Re_{\alpha\alpha})=\partial^2(\rho_{12}\varepsilon_{\alpha\alpha}+\rho_{22}e_{\alpha\alpha})/\partial t^2 - \beta f F_{(\nu)}\,\partial(\varepsilon_{\alpha\alpha}-e_{\alpha\alpha})/\partial t, \quad (2)$$

where ε_{ij} is the solid strain tensor, $e_{\alpha\alpha}$ is the trace of the liquid strain tensor, β is the pore volume fraction (equating the fluid volume fraction), and ρ_{11}, ρ_{12}, and ρ_{22} are the mass density parameters for the hydrogel that are related to the solid and fluid mass densities ρ_s and ρ_f, respectively, by the identities

$$\rho_{11}+\rho_{12}=(1-\beta)\rho_s,$$

$$\rho_{12}+\rho_{22}=\beta\rho_f,$$

$$\rho_{12}=(1-\alpha)\beta\rho_f,$$

where $\alpha>1$ is a molecular shape factor which is independent of the solid or fluid mass densities. For a matrix built up by spherical particles, Berryman[34] showed to be $\alpha=\frac{1}{2}(\beta^{-1}+1)$.

Furthermore, ρ_{11} is the inertial mass density of the solid matrix when it accelerates while the fluid is contemporarily prevented to move, and ρ_{12} is the mass density parameter for the force that the fluid exerts on the solid as the latter is accelerated relative to the former.[23] This happens since the fluid and the solid in the poroelastic media are coupled to each other. If fluid and solid would be independent of each other (i.e., $\rho_{12}=0$) the inertial mass density of solid and fluid in the bi-phasic medium would result just equal to their specific ones (ρ_s and ρ_f) multiplied by their volume fractions $(1-\beta)$ and β, respectively.

Moreover, P, Q, and R are the poroelastic coefficients of the medium that can be measured by means of jacketed and unjacketed experiments.[24] In the jacketed rheological measurements, the solid matrix is subject to compressional tests carried out maintaining the pore fluid at constant pressure, while in the unjacketed ones, the specimen dilatation is measured as a function of the fluid pressure in the pores, leaving the solid matrix free from external forces.[24]

In the limit of high liquid phase content ($\beta\approx1$) and incompressible constituents, the following conditions over the poroelastic coefficients and mass density parameters hold:[16,17,23]

$$R\gg Q\gg P, \quad (3)$$

$$Q/R\cong(1-\beta)/\beta\cong(1-\beta), \quad (4)$$

$$\rho_{12}=-\rho_{11}\ll\rho_{22} \quad (5)$$

By introducing the above approximations into the longitudinal wave equations we obtain

$$\nabla^2Qe_{\alpha\alpha}=\partial^2\rho_{11}(\varepsilon_{\alpha\alpha}-e_{\alpha\alpha})/\partial t^2+\beta f F_{(\nu)}\,\partial(\varepsilon_{\alpha\alpha}-e_{\alpha\alpha})/\partial t, \quad (6)$$

$$\nabla^2(Q\varepsilon_{\alpha\alpha}+Re_{\alpha\alpha})=\partial^2(\rho_{12}\varepsilon_{\alpha\alpha}+\rho_{22}e_{\alpha\alpha})/\partial t^2 - \beta f F_{(\nu)}\,\partial(\varepsilon_{\alpha\alpha}-e_{\alpha\alpha})/\partial t. \quad (7)$$

Given that the friction coefficient f is very high[25,27,30–33] it follows that the displacement $|\varepsilon_{\alpha\alpha}-e_{\alpha\alpha}|$ of the "slow" wave (liquid and solid in counter-phase) is very small compared to that of the fast wave $|e_{\alpha\alpha}|$ so that it is possible to pose $|\varepsilon_{\alpha\alpha}|\approx|e_{\alpha\alpha}|$ and, hence

$$(\rho_{12}\varepsilon_{\alpha\alpha}+\rho_{22}e_{\alpha\alpha})\cong(\rho_{22}+\rho_{12})e_{\alpha\alpha}=\beta\rho_f e_{\alpha\alpha}, \quad (8)$$

$$(Q\varepsilon_{\alpha\alpha}+Re_{\alpha\alpha})\cong(R/\beta)e_{\alpha\alpha} \quad (9)$$

that introduced in Eq. (7) leads to

$$\nabla^2\frac{R}{\beta}e_{\alpha\alpha}\cong\partial^2(\beta\rho_f e_{\alpha\alpha})/\partial t^2-\beta f F_{(\nu)}\,\partial(\varepsilon_{\alpha\alpha}-e_{\alpha\alpha})/\partial t. \quad (10)$$

Assuming for dilute matrices Berryman's[34] formula (that calculates ρ_{11} for coil-like polymer molecules as those ones of the PVA hydrogel), ρ_{11} reads

$$\rho_{11}=(1-\beta)\rho_s-\tfrac{1}{2}(1-\beta^{-1})\beta\rho_f$$

from where for $\beta\cong1$ it follows that $\rho_{11}\cong0$. Hence, Eqs. (6) and (10) approximately read as

$$\nabla^2Qe_{\alpha\alpha}\cong\beta f F_{(\nu)}\,\partial(\varepsilon_{\alpha\alpha}-e_{\alpha\alpha})/\partial t, \quad (11)$$

$$\nabla^2\frac{R}{\beta}e_{\alpha\alpha}\cong\partial^2(\beta\rho_f e_{\alpha\alpha})/\partial t^2. \quad (12)$$

Moreover, by introducing Eq. (12) into Eq. (11), the following relation between the "slow wave" and the fast wave displacements,

$$F(\nu)\frac{\partial(\varepsilon_{\alpha\alpha}-e_{\alpha\alpha})}{\partial t}\cong\frac{1}{f}\frac{Q}{R}\frac{\partial^2(\beta\rho_f e_{\alpha\alpha})}{\partial t^2}, \quad (13)$$

is obtained.

Finally, by introducing Eq. (13) into Eq. (10), at first order in $(1-\beta)$, we obtain

$$\nabla^2\frac{R}{\beta}e_{\alpha\alpha}\cong\beta\partial^2(\beta\rho_f e_{\alpha\alpha})/\partial t^2 \quad (14)$$

that, under the hypothesis of β constant, reads

$$\nabla^2Re_{\alpha\alpha}\cong\beta^3\partial^2(\rho_f e_{\alpha\alpha})/\partial t^2. \quad (15)$$

Equation (15) represents a purely elastic wave of the first type that propagates in a medium with a speed c according to the law

$$c^2=R/(\rho_f\beta^3)\approx c_f^2/\beta^3, \quad (16)$$

where c_f is the wave velocity in the fluid phase. Since β is smaller than but close to 1 in Eq. (16) we can observe that, in dilute poroelastic media, the compressional wave has a velocity that is close but always higher than that one in the pure fluid phase.

Since Eq. (14) is a completely elastic wave equation, to take into account for the US energy dissipation, the highest

order of approximation must be considered. In order to do that, we put Eq. (6) into Eq. (10) and, with the help of Eq. (4), we obtain the wave equation

$$\nabla^2 \frac{R}{\beta} e_{\alpha\alpha} \cong \beta \partial^2(\beta \rho_f e_{\alpha\alpha})/\partial t^2 + (1-\beta) \times (\rho_{11}/\beta f F_{(\nu)}) \partial^3(\rho_f e_{\alpha\alpha})\, \partial t^3. \quad (17)$$

1. Phase velocity and attenuation of "fast" plane wave

Equation (17) for plane waves $e_{aa} \propto e^{-\alpha x} e^{i(kx-\omega t)}$ gives the characteristic equation

$$(k+i\alpha)^2 = \omega^2 \rho_f (\beta^3/R)[1 - i\omega(Q/R)(\rho_{11}/fF_{(\nu)})]. \quad (18)$$

By solving k and α and by using the purely elastic phase velocity $c_0^2 = R/\rho_f \beta^2$, the speed and the attenuation per cycle are obtained, respectively, to be

$$c^2 = c_0^2(1 + \alpha^2/k^2), \quad (19)$$

$$2\pi\alpha/k = -\pi(c/c_0)^2 \omega(1-\beta)(\rho_{11}/\beta f F_{(\omega)}). \quad (20)$$

B. Compressional fast wave in hydrogels

Introducing a new constituent such as the bounded water, we must pay attention to the definition of the fluid volume fraction of the hydrogel.

Since the bounded water phase is not a fluid phase, it must be subtracted from the water volume fraction β that is the total volume fraction of the water.

The effective free water volume fraction β_e can be obtained on the hypothesis that the number of bounded water molecules is proportional to the polymer-water contacts.

Since the probability of a polymer-polymer contact at very low polymer concentration [near $\beta \approx 1$, let us say for $(1-\Delta) \ll \beta < 1$] is practically null, the bounded water volume fraction β_{bw} is proportional to the polymer volume fraction $(1-\beta)$ in that range.

When the polymer concentration is high [let us say for $0 < \beta \ll (1-\Delta)$], where Δ represents the parameter that marks the boundary between the two regimes, due to the high probability of polymer-polymer contacts, the increase in polymer content does not cause a proportional increase in bounded water so that β_{bw} must approach a constant value ϕ as β goes to zero.

If we approximate the approaching of the bounded water volume fraction to this constant value ϕ by means of an exponential law, we can write

$$\beta_{\mathrm{bw}} = \phi(1 - \exp[-(1-\beta)/\Delta]), \quad (21)$$

where $0 < \Delta < 1$ and $0 < \phi < 1$ are empirical parameters to be deduced from the experimental data.

Therefore, the free water volume fraction reads as

$$\beta_e = \beta - \phi(1 - \exp[-(1-\beta)/\Delta]). \quad (22)$$

By introducing the free water volume fraction β_e, the pure elastic acoustic fast wave (15) and its speed, respectively, read as

$$\nabla^2 R e_{\alpha\alpha} \cong \beta_e^3 \partial^2(\rho_f e_{\alpha\alpha})/\partial t^2, \quad (23)$$

$$c_0^2 \cong \frac{c_f^2}{(\beta - \phi(1 - \exp[-(1-\beta)/\Delta]))^3}, \quad (24)$$

where $c_0 = (R/\rho_f \beta_e^3)^{1/2}$ is the pure elastic longitudinal wave velocity, $c_f = (R/\rho_f)^{1/2}$ its velocity in the intermolecular fluid (free water), R is Biot's compressional modulus of the fluid,[16,21] and $e_{\alpha\alpha}$ is the trace of the free water stress tensor.

It is worth noting that for vanishing Δ and for $\beta \leq (1-\varepsilon)$, where $\varepsilon \gg \Delta$ is a positive number (smaller than 1), it holds that $\beta_{\mathrm{bw}} \cong \phi$, $\beta_e \cong (\beta - \phi)$, and Eq. (24) leads to the relation

$$c_{0(\beta)}^2 \cong \frac{c_f^2}{(\beta - \phi)^3}. \quad (25)$$

Therefore, the amount of bounded water ϕ can be evaluated by means of the best-fitted value $\lim_{\beta \to 1} c_{0(\beta)}$ of the experimental data $c_{0(\beta_{(i)})}$ for $\beta_{(i)} \leq (1-\varepsilon)$ following the equation

$$\phi = 1 - \left(\frac{c_f}{\lim\limits_{\beta \to 1} c_{0(\beta)}} \right)^{2/3}. \quad (26)$$

It is noteworthy to note that the presence of the bounded water generates a velocity gap between the US velocity in pure water and that one extrapolated for hydrogels at $\beta = 1$ (a hydrogel made up by 100% of water).

1. Bounded water-polymer network viscoelastic interaction

The bounded water-polymer network viscoelastic interaction can be introduced in the poroelastic equations by adding to Biot's viscous force (with $F_{(\nu)} = 1$)

$$\beta_e f\, \partial(e^*_{\alpha\alpha} - e_{\alpha\alpha})/\partial t, \quad (27)$$

the viscoelastic one due to the bounded water

$$\eta_{(\nu)}\, \partial(\varepsilon_{\alpha\alpha} - e^*_{\alpha\alpha})/\partial t + \kappa(\varepsilon_{\alpha\alpha} - e^*_{\alpha\alpha}), \quad (28)$$

where $e^*_{\alpha\alpha}$ is the trace of the bounded water stress tensor.

Actually, introducing the bounded water stress tensor variable, the bi-phasic approach disembogues into a three-phasic one that is out of the purpose of this work. Nevertheless, the bi-phasic model can be retained since the bounded water mass density is not much different from that one of the polymer. It is much like the bounded water "inflates" the polymer chains, creating a bearing around them. In this case, the bi-phasic medium can be conceived composed of the "polymer-bounded water aggregate," as matrix, plus the interstitial free water. Thence it is possible to introduce the following approximations.

(i) The mass density of the solid aggregate approximates that one of the polymer.
(ii) The trace of the strain tensor of the polymer $\varepsilon_{\alpha\alpha}$ approximates that one of the solid aggregate.
(iii) P, Q, and R are the poroelastic coefficients of the new bi-phasic medium. Moreover, since not the whole bounded water is involved in the fluid-solid shear process.

(iv) The inertial effect of bounded water involved in the fluid-solid shear process can be disregarded.

By means of the fourth hypothesis, the force between the free water and the bounded water can be equated to that one between the bounded water and the polymer matrix, leading to the additional equation needed to solve the three stresses that reads

$$\beta_e f F_{(\nu)}\,\partial(e^*_{\alpha\alpha}-e_{\alpha\alpha})/\partial t=\eta_{(\nu)}\,\partial(\varepsilon_{\alpha\alpha}-e^*_{\alpha\alpha})/\partial t+\kappa(\varepsilon_{\alpha\alpha}-e^*_{\alpha\alpha}). \tag{29}$$

Moreover, under hypotheses (i)–(iii) the system of poroelastic equations (1) and (2) reads as

$$\nabla^2(P\varepsilon_{\alpha\alpha}+Qe_{\alpha\alpha})=\partial^2(\rho_{11}\varepsilon_{\alpha\alpha}+\rho_{12}e_{\alpha\alpha})/\partial t^2+\beta f\,\partial(e^*_{\alpha\alpha}-e_{\alpha\alpha})/\partial t, \tag{30}$$

$$\nabla^2(Q\varepsilon_{\alpha\alpha}+Re_{\alpha\alpha})=\partial^2(\rho_{12}\varepsilon_{\alpha\alpha}+\rho_{22}e_{\alpha\alpha})/\partial t^2-\beta f\,\partial(e^*_{\alpha\alpha}-e_{\alpha\alpha})/\partial t. \tag{31}$$

In dilute bi-phasic media the compressional plane wave of interstitial fluid, $e_{\alpha\alpha}\propto e^{-\alpha x}e^{i(kx-\omega t)}$, induces a planar slow wave, as shown in Eq. (13), that leads to

$$(\varepsilon_{\alpha\alpha}-e_{\alpha\alpha})=-(i\omega Q\beta_e{}^2/Rf)e_{\alpha\alpha},$$

where $\omega=2\pi\nu$.

In this case Eq. (29) reads as

$$\beta_e f\,\partial(e^*_{\alpha\alpha}-e_{\alpha\alpha})/\partial t=(\eta_{(\nu)}+j(\kappa/\omega))\,\partial(\varepsilon_{\alpha\alpha}-e^*_{\alpha\alpha})/\partial t, \tag{32}$$

leading after simple manipulation to the relation

$$\partial(\varepsilon_{\alpha\alpha}-e_{\alpha\alpha})/\partial t=\{(\beta_e f+\eta_{(\nu)}+j(\kappa/\omega))/(\eta_{(\nu)}+j(\kappa/\omega))\}\,\partial(e^*_{\alpha\alpha}-e_{\alpha\alpha})/\partial t, \tag{33}$$

where that can be recast as

$$\beta_e f\,\partial(e^*_{\alpha\alpha}-e_{\alpha\alpha})/\partial t=F^*_{(\omega)}\,\partial(\varepsilon_{\alpha\alpha}-e_{\alpha\alpha})/\partial t, \tag{34}$$

where the complex "friction" coefficient $F^*_{(\omega)}$ reads as

$$F^*_{(\omega)}=[(\beta_e f)^{-1}+(\eta_{(\nu)}+j(\kappa/\omega))^{-1}]^{-1}. \tag{35}$$

Hence, by introducing Eq. (34) into Eqs. (30) and (31) for plane waves, the dilute matrix equation (17) reads as

$$\nabla^2\frac{R}{\beta}e_{\alpha\alpha}\cong\beta\partial^2(\beta\rho_f e_{\alpha\alpha})/\partial t^2+(1-\beta)\times(\rho_{11}/F^*_{(\omega)})\partial^3(\rho_f e_{\alpha\alpha})/\partial t^3 \tag{36}$$

so that for the fast plane wave $e_{\alpha\alpha}\propto e^{-\alpha x}e^{i(kx-\omega t)}$ it leads to the characteristic equation

$$(k+i\alpha)^2=\omega^2\rho_f(\beta_e{}^3/R)[1-i\omega(1-\beta_e)(\rho_{11}/F^*_{(\omega)})] \tag{37}$$

that solved in α and c gives

$$c^2=c_0^2\left(1+\alpha^2/k^2\right)\Big/\left[1+(1-\beta_e)\omega\rho_{11}\,\mathrm{Im}\{F^{*-1}_{(\omega)}\}/\beta_e{}^2\right], \tag{38}$$

$$\alpha/k=-1/2(c/c_0)^2\omega(1-\beta_e)\rho_{11}\,\mathrm{Re}\{F^{*-1}_{(\omega)}\}, \tag{39}$$

where

$$\mathrm{Re}\{F^{*-1}_{(\omega)}\}=[\eta_{(\omega)}(1+\eta_{(\nu)}/\beta_e f)+(\kappa^2/\beta_e f\omega^2)]/(\eta_{(\nu)}{}^2+(\kappa/\omega)^2), \tag{40}$$

$$\mathrm{Im}\{F^{*-1}_{(\omega)}\}=-(\kappa/\omega)/(\eta_{(\nu)}{}^2+(\kappa/\omega)^2). \tag{41}$$

In the following we consider the case when the bounded water-network interaction is prevalently viscous such as

$$\eta>(\kappa\rho_{\mathrm{bw}})^{1/2}, \tag{42}$$

where ρ_{bw} is the mass density of the bounded water that we assume close to that of free water ρ_f.

At high frequencies such $\omega>\omega_g=(2\pi\eta/\rho_f)>(\kappa/\rho_{\mathrm{bw}})^{1/2}$ (far away from bounded water resonance) hence, it holds that

$$\kappa/\omega\eta\ll\kappa/\omega_g\eta<1. \tag{43}$$

Moreover, in order that the crossover frequency $\nu_g=\eta/\rho_f$ is much smaller than the unattainable Biot's one $\nu_c=f/\rho_{f'}$ in the high frequency limit, it must hold

$$\lim_{\nu\to\infty}\eta_{(\nu)}\ll f. \tag{44}$$

If the high frequency behavior of the bounded water viscosity $\eta_{(\nu)}$ is modeled by a dimensionless coefficient as

$$\eta_{(\nu)}=\eta_0(\omega_g/\omega)^{\delta}, \tag{45}$$

it follows that $\omega_g=2\pi\nu_g=2\pi\eta_{(\nu=\nu_g)}/\rho_f=2\pi\eta_0/\rho_{f'}$ and that conditions (43) and (44) hold contemporarily by requiring $0<\delta\leq 1$. In such a case, by introducing them into Eqs. (40) and (41) it follows that

$$\lim_{\omega/\omega_g\gg 1}\mathrm{Re}\{F^{*-1}_{(\omega)}\}\cong(\kappa/\omega\eta)^2+[(1+\eta_{(\nu)}/\beta_e f)/\eta_{(\nu)}]\cong 1/\eta_{(\nu)}, \tag{46}$$

$$\lim_{\omega/\omega_g\gg 1}\mathrm{Im}\{F^{*-1}_{(\omega)}\}\cong 0, \tag{47}$$

where $\nu=2\pi/\omega$. Equations (46) and (47) introduced into Eq. (38), in a dilute polymer hydrogel ($\beta\approx 1$ and $\rho_{11}\ll 1$), lead to

$$c^2=c_0^2(1+\alpha^2/k^2)\cong c_0^2, \tag{48}$$

being typically $(\alpha/\kappa)^2$ very small (of order of 10^{-3} in our experiments) and to the specific US attenuation per cycle

$$2\pi\alpha/k\approx-\pi(c/c_0)^2(\omega/\omega_g)^{1+\delta}(1-\beta+\phi(1-\exp[-(1-\beta)/\Delta])\sigma_{pf}, \tag{49}$$

where $\sigma_{pf}=\rho_{11}/\rho_f$.

For hydrogels with small Δ, and for $(1-\beta)/\Delta\gg 1$, finally, Eq. (49) leads to

$$2\pi\alpha/k\approx-\pi(c/c_0)^2(\omega/\omega_g)^{1+\delta}(1-\beta+\phi)\sigma_{pf}. \tag{50}$$

From Fig. 1, that shows the acoustic US fast wave absorption, it can be observed that the bounded water raises the linear behavior, while Δ smooths the curve in the interval $1-\Delta>\beta>1$.

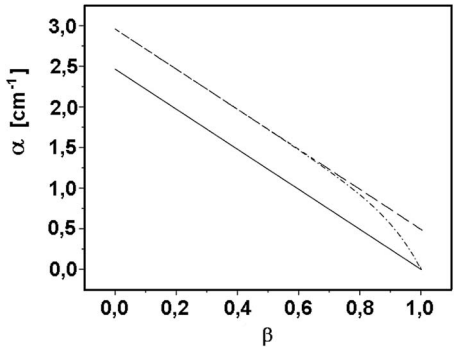

FIG. 1. Theoretical behavior of acoustic US fast wave absorption in a hydrogel given by Eq. (52) as a function of the water volume fraction for various values of the parameters: $\phi=0$ and $\Delta=0$ (full line), $\phi=0.2$ and $\Delta=0.0006$ (dashed line), and $\phi=0.2$ and $\Delta=0.1$ (dashed-dotted line).

From Fig. 2, depicting the theoretical behavior of the acoustic speed of US fast wave, it can be seen that

(i) the bounded water leads to an upward shift in the wave speed,
(ii) that Δ smooths the curve upward in the region $1-\Delta<\beta<1$, and
(iii) when $\Delta \ll 1$ there is a speed jump at $\beta \cong 1$.

C. High polymer concentration

The characteristic equation for slow and fast plane waves stemming from Eqs. (30) and (31) turns out to be formally the same as that one given by Biot[17] where the friction term $\beta f F_{(\nu)}$ is substituted by $F^*_{(\omega)}$ [see Eq. (34)] that at high frequency is given by Eqs. (46) and (47).

Nevertheless, it must be observed that Biot's[17] model assumes that the poroelastic coefficients are constants (or at least very smoothly varying) while in hydrogels they actually may change very much when they are partially dried up.[33]

Moreover, since we wish both to build up a model that can be applied to biological tissues, where the solid concentration as well as that one of the bounded water can be very high (up to 60%), and to improve the experimental fitting of data beyond the range of validity of the dilute matrix approximation at intermediate water volume fraction values (but not to validate the model), we opt for a more direct semi-empirical approach.

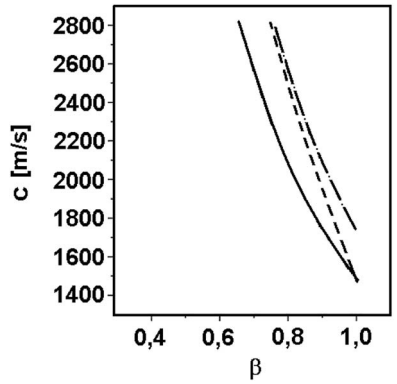

FIG. 2. Theoretical behavior of the acoustic speed of propagation of US fast wave in a hydrogel given by Eq. (24) as a function of the water volume fraction for various values of the parameters: $\phi=0$ and $\Delta=0$ (full line), $\phi=0.1$ and $\Delta=0$ (dashed line), and $\phi=0.1$ and $\Delta=0.1$ (dashed-dotted line).

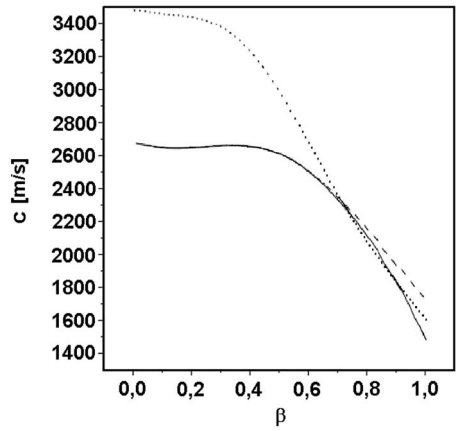

FIG. 3. Theoretical behavior of the acoustic speed of propagation of US fast wave in a hydrogel given by Eq. (52) as a function of the water volume fraction for various values of the parameters: $\phi=0.1$, $\Delta=0$, $\gamma=0.7$, and $\chi=-0.4$ (dashed line); $\phi=0.1$, $\Delta=0.1$, $\gamma=0.7$, and $\chi=-0.4$ (full line); $\phi=0.031$, $\Delta=0$, $\gamma=0.44$, and $\chi=-0.25$ (dotted line).

In order to do that, we observe that for vanishing $\beta=0$ values, the speed of propagation of the US is finite and equal to that of polymeric solid c_s, while the law (24) diverges to infinity at $\beta=\phi$ and gives negative values for $\beta=0$.

The contribution that cancels the divergence of the denominator of Eq. (24) (let us call it $G_{(\beta)}$ in the dilute matrix approximation) can be put in the form

$$c^2 = \frac{c_f^2}{(\beta - \phi(1-\exp[-(1-\beta)/\Delta]))^3 + G_{(\beta)}}, \tag{51}$$

where the conditions required to $G_{(\beta)}$ are

$$\lim_{\beta\to 1} G_{(\beta)} = 0,$$

$$\lim_{\beta\to 0} G_{(\beta)} > 0.$$

For this reason it is appropriate to use the series approximation

$$G(\beta) = \gamma(1-\beta) + \chi(1-\beta)^2 \quad \text{with} \quad \gamma+\chi>0$$

that in Eq. (29) leads to

$$c^2 = \frac{c_f^2}{(\beta - \phi(1-\exp[-(1-\beta)/\Delta]))^3 + \gamma(1-\beta) + \chi(1-\beta)^2} \tag{52}$$

and that for $(1-\beta)/\Delta \gg 1$ gives

$$c^2 = \frac{c_f^2}{(\beta-\phi)^3 + \gamma(1-\beta) + \chi(1-\beta)^2}. \tag{53}$$

From Fig. 3 we can see the change in the US wave speed following the introduction of the polynomial expression $G_{(\beta)}$: the polymer network cancels the divergence of US speed at $(\beta-\phi)=0$ and lowers it at the intermediate values of β in a progressive manner.

Finally, for β close to 1 we observe that the increase in the bounded water in Eq. (53) increments the US speed through the term $(\beta-\phi)^3$ while the elasticity of the polymer network lowers it mainly through the vanishing term $\gamma(1-\beta)$ (if $\gamma>0$).

III. EXPERIMENTAL

A. Materials and methods

Gel samples were prepared in parallelepipeds of $2\times2\times1$ cm^3 using PVA with a degree of hydrolysis of 99+% and an average molecular weight of 115.000 ± 30.000 (Aldrich, Milan, Italy) dissolved into de-ionized water in a concentration of 10% by weight. The homogeneous solution was refrigerated at -80 °C starting from room temperature 23 ± 1 °C. The freezing-thawing procedure was repeated two, three, four, and six times. The samples were left to equilibrate in de-ionized water for 72 h.

The experimental tests were carried out at different hydration conditions down to a minimum of about 50%, taking care that the drying was gradual and homogeneous.

The reversibility of the de-hydration treatment was checked at the end after the drying steps.

The ultrasonic pulses were generated by a Panametrics® Pulser model 5052PR (Waltham, MA) coupled with a polyvinylidene fluoride piezoelectric transducer assembled in our laboratory following the procedure of Naganishi *et al.*[35]

A cylindrical chamber immersed in a water bath constitutes the experimental cell. The US transducer/receiver is fixed on a planar side-wall. An inner flat counter-wall, free to translate inside the cylinder and put in contact with the back surface of the samples, is used as reflecting surface.

The ultrasonic disk-like transducer used in the experiment has an aperture size of 1.5 cm. The measurements are carried out in the near field condition with the front surface of the gel samples in contact with the transducer surface. All the volume in front of the transducer is occupied by the sample (so that there is no problem about US focalization) and US echoes are very well detected up to 10 cm far apart from the transducer.

The Pulser voltage spike of -270 V induces an ultrasonic pulse of 250 kHz of frequency through the transducer.

The distance between the transducer and the reflecting stainless steel layer behind the samples was measured with an accuracy of ±0.01 cm and maintained constant through the whole experiment.

Echo signal registration and conditioning data were collected with a routine and carried out with the LABVIEW™ software on a computer through a National Instruments® data acquisition device.

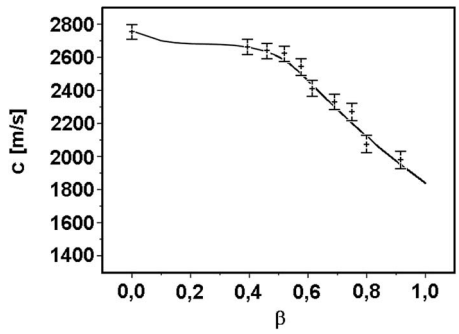

FIG. 4. Experimental acoustic US speed of propagation of fast wave in PVA hydrogels, with best fit (full line), as a function of the water volume fraction $(0<\beta<1)$ for a hydrogel sample obtained by means of 2 cycles of cross-linking.

Finally, the samples were totally dehydrated in an oven at 40 °C with desiccant silica gels to measure their polymer content and the US speed in the dry solid.

The US absorption coefficient α was deduced by using the mathematical relation $\alpha=(1/2d)\ln(A_0/A_{(2d)})$, where A_0 and $A_{(2d)}$ represent both the initial and final wave amplitudes, respectively, and where d is the sample thickness.

The water volume fraction of the hydrogel samples β was obtained by means of the respective weight fractions P_w and P_p such as $\beta\approx P_w/(P_w+P_p)$ since the water and PVA specific densities are very close to each other.

After the samples were left to fully hydrate themselves in distilled water, the fractional water volume was measured to be $\beta=0.917\pm0.001$ for all the samples.

The fitting of the experimental results was carried out by means of a multiple parameter best fit utilizing an appropriate routine in MATLAB® 7.0.

The error bars are obtained both from theoretical calculation (taking into account all the experimental errors in space, time, and temperature) and from experimental evaluation. The mean square root deviation of data resulted much smaller than the theoretical errors.

B. Ultrasound phase velocity

Experimental data of US wave speed with the best-fitted curve are shown in Fig. 4 for the hydrogel sample submitted to 2 cycles of cross-linking. The most probable values of the model parameters for all samples are given in Table I.

TABLE I. Most probable values of the model parameters ϕ, Δ, γ, χ, and $\gamma+\chi$ obtained from the best fit of the experimental data by means of expression (31) as a function of the number of cross-linking cycles (first column).

Number of cross-linking cycles	ϕ	Δ	γ	χ	$\gamma+\chi$	$\lim_{\beta\to1} c$ (m s^{-1})	c_s (m s^{-1})
2	0.131	0.0006	0.742	−0.453	0.289	1830	2755
3	0.075	0.0006	0.570	−0.363	0.206	1667	3266
4	0.063	0.0006	0.445	−0.247	0.197	1636	3339
6	0.020	0.0006	0.307	−0.109	0.198	1528	3340

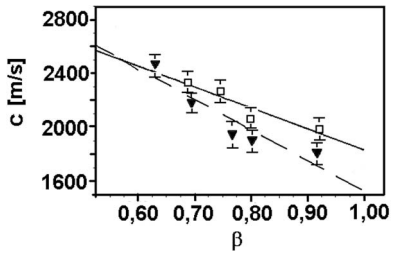

FIG. 5. Experimental acoustic US speed of propagation of fast wave in PVA hydrogels as a function of the water volume fraction at various degrees of polymer matrix cross-linking: 2 cycles (⊡) and 6 cycles (▽) of cross-linking, with the best fit (dashed line and full line, respectively). In this case, the detail of the US speed behavior for high water volume fraction values ($0.6<\beta<1$) is shown.

From Fig. 4 we can see that at intermediate values of β, the US wave speed progressively departs from the model dependence $(\beta-\phi)^{-3/2}$ toward the value of the dry solid polymer in agreement with the theoretical behavior (52) shown in Fig. 3. The measurements show that the effect of the polymer matrix starts to influence the US speed of propagation for values of β as high as 0.8.

For β close to zero, the US speed of propagation converges to the speed of the dry polymer which rises when the number of cross-linking cycles increases because of the greater polymer stiffness, as shown in Table I.

For β equal to 1, the US speed is extrapolated by means of a best-fit procedure and reported in Table I. The data referring to the samples with 2 and 6 cycles of cross-linking have been reported in Fig. 5. The data show that the US phase velocity is sensibly higher than that of pure water (that in our experimental condition has been measured to be 1483 m/s). In Fig. 6 the bounded water volume fraction ϕ is shown as a function of the number of cross-linking cycles of the sample. The evaluation of ϕ is obtained by introducing into Eq. (26), being $\Delta\cong 0$, the limiting velocity values of Table I. The bounded water volume fraction ϕ ranges from 2% in the PVA samples with six cross-linking cycles to 13% for the PVA samples with two cross-linking cycles.

As shown in Table I, we can observe that the lower the gap speed at $\beta=1$, the bigger the number of the cross-linking cycles and the lower the measured bounded water fraction ϕ present in the hydrogel. This agrees with the characteristics of PVA hydrogel synthesized by means of freezing-thawing

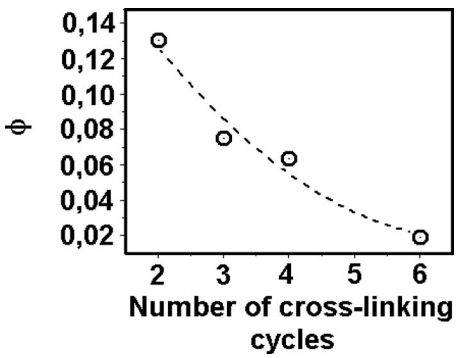

FIG. 6. Estimated bounded water fraction in PVA hydrogel as a function of the number of cross-linking cycles.

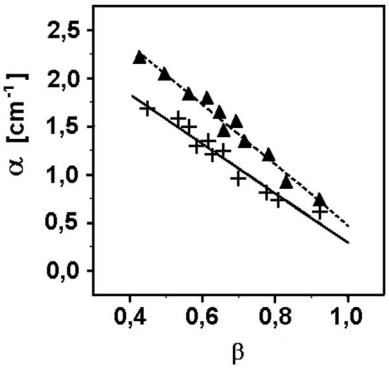

FIG. 7. Experimental acoustic US fast wave attenuation in PVA hydrogels as a function of the water volume fraction at various degrees of polymer matrix cross-linking: 4 cycles (▲) and 6 cycles (+) of cross-linking with best fit (dashed-dotted line and dotted line, respectively).

cycles where the number of polymer-polymer contacts (cross-links) grows as the number of freezing-thawing cycles increases.[36] Moreover, since lower values of ϕ in samples with higher cross-linking correspond to lower values of the US speed, this behavior cannot be ascribed to the elasticity of the polymer network that leads to a variation in opposite sign.

In fact, as shown in Table I, both γ and $(\gamma+\chi)$ (that account for the effect of the polymer network elasticity on the US speed [γ contributes prevailing in the region of high $\beta\approx 1$, while $(\gamma+\chi)$ in the region of small $\beta\approx 0$]) decrease as the network cross-linking increases so that by looking at Eq. (53) it comes clearly out that in such a case they would cause an increase in the US speed.

Moreover, since both γ and $(\gamma+\chi)$ are positive for the intermediate values of β, the effect of the polymer network is to decrease the US speed and to eliminate the US speed divergence due to the dilute matrix approximation for small values of β.

From experimental data we can also see that the value of the parameter Δ obtained from the last square fit procedure is equal to 0.0006 (practically null) for all PVA gel samples so that ϕ effectively represents the bounded water concentration and $(\beta-\phi)$ the free water concentration. This fact says that the bounded water concentration remains practically unchanged inside the PVA gel samples (as a function of β) so that primarily free water is subtracted when they are (mildly) dried.

C. Ultrasound wave attenuation

Some of the experimental data as well as the fits of the theoretical expression (49) are shown in Fig. 7. For the attenuation measurements as well as for the velocity ones, the value of the fitted parameter Δ resulted practically null.

A linear decrease in the US wave attenuation α is measured as a function of β for all samples with a mean value $\partial\alpha/\partial\beta=-2.4\pm 0.4$ cm^{-1}.

The pure water attenuation has also been measured to be 0.022 cm^{-1} and found to be much smaller than that one of the gel in the order of 1 cm^{-1}.

IV. DISCUSSION

The US propagation in natural hydrogels and soft tissues is currently described by a single-phase wave equation[37,38] where the medium is conceived as a fluid "solution" in which dissolved molecules can introduce processes of both dissipation and resonance. Even if this scheme completely ignores the liquid-solid arrangement, it gives appreciable results that are able to explain many aspects of tissue acoustical behavior. This probably happens because of the high built-in flexibility of such an equation that is able to comprehend a wide class of acoustical media thanks to a number of parameters that can be empirically adjusted to describe the propagation of acoustic waves.

Yang and Cleveland[39] showed that it is possible to reproduce the frequency dependence of the absorption with an exponent equal to 1.1 by supposing two juxtaposed relaxing processes that may or may not be real. In this way some information about the material medium (e.g., a natural gel or a tissue) is lost from the US behavior.

The model presented here discloses how the behavior of the US propagation is linked to the arrangement of the solid and liquid phases of the medium.

More recently Kowalski[40] developed a theory for the propagation of US in a dilute suspension. Even if conceptually different from a polymeric gel, a fluid suspension can be assimilated to a bi-phasic medium with a solid matrix (with its own elasticity and permeability) and a fluid that permeates the interstices. Obviously, the Kowalski model is expressed in terms of the viscoelastic parameters of the suspension that do not correspond *tout court* to those of the bi-phasic approach, except for the fluid fraction volume β.

The theoretical dependence of the US velocity as a function of the water volume fraction found by Kowalski is of the same type obtained in the present paper with the same good experimental agreement. The main difference is that the suspension does not have bounded water (i.e., $\phi=0$) so that at $\beta=1$ the US speed converges to that of the pure fluid.

Hence, the following features of the US propagation in hydrogels can be ascribed to their state of aggregation.

(i) The speed of propagation of US in highly hydrated gels is always a little bit higher than that of water (1480 m/s) since in Eq. (26) $\beta<1$ and $\phi>0$.

(ii) The US specific attenuation $2\pi\alpha/\kappa$ in natural hydrogels can follow a non-integer frequency law $\nu^{(1+\delta)}$ with $0<\delta\leq 1$, where δ is the exponent of the polymer-bounded water viscous interaction.

This outcome well agrees with the attenuation data of US in natural gels where δ is typically about 0.25–0.50 while the value for pure water is 1.

As far as it concerns the applicability of the diluted matrix approximation, we observe that the polymer content sensibly influences the US wave speed up to values of β as high as 0.7. For β higher than 0.70 the polymer effect on the US speed becomes smaller and smaller and the behavior approaches that one of dilute gels depicted in Fig. 1. By using Eq. (53) for $\beta=0.917$, the variation in the US speed due to the polymer network can be evaluated to be about 3.5% (for the PVA samples submitted to four cross-linking cycles) with a maximum value of 5.2% for the samples submitted to two cross-linking cycles.

It must also be noted that the development of tissue-mimicking US phantoms can take advantage by a model that discloses the relation between the medium organization and the US behavior.

In principle, even though living tissues, or organs, have their own complex morphology and anisotropy, a simplified bi-phasic model of soft (isotropic) natural tissue can be conceived by modeling biological cells as poroelastic spheres, endowed by internal and superficial elasticity and permeability, dispersed in a hydrogel environment.

Although the polymer and the bounded water contents of living tissues can reach much higher concentrations than in PVA gels, the present model can be used to describe the behavior of each type of biological hydrogel of a soft tissue (e.g., extra-cellular matrix, internal body of the cell, and so on). In this case, the "free water fractional content" is given by the effective β [given by Eq. (22) with $\Delta=0$] while the polymer-bounded water aggregate constitutes the solid part of the hydrogel matrix.

Even considering this simplest case, there are some limitations derived from the increased complexity of the architecture of the medium. First of all, in order to maintain the continuum approach, the US wave must not resolve the structure of the single cell. As a consequence of this, the theory is limited to US frequencies whose wavelength is much bigger than the cell dimensions. For instance, for cells of order of 30 μm and wave speed of order of 2×10^3 m/s, the upper frequency limit for the theory is smaller than 66 MHz.

It must also be pointed out that the number of material parameters of the model increases. In addition to β and f of the extra-cellular medium, the model would require β and f of the inner volume of the cells, the superficial elasticity as well as permeability of their membrane, and the percentage of the cellular volume. Such a relatively large number of material parameters will give rise to many possible tissue configurations. In this case, the major problem is to identify the appropriate set of values of those coefficients for each real tissue and how experimentally to measure them. Although the complexity of the model increases, it can definitely describe the US propagation in terms of collective cells and extra-cellular matrix poroelastic characteristics.

This opens up the way to US non-invasive tissue physiology evaluation since the permeability and elasticity of the cell structures depend on their state and functionality.

Once the model is validated, then it could be refined by introducing capillaries and blood vessels in the tissue as tubes filled by fluid (with their own internal β and wall elasticity and permeability).

V. CONCLUSIONS

In the present work a continuum model for US acoustic longitudinal waves in hydrogels has been presented. The model shows that a speed gap, at the hydrogel water volume fraction $\beta=1$, is generated by the presence of the bounded

water around the hydrogel polymer matrix: the bigger the bounded water concentration, the higher the US speed gap at $\beta=1$.

The poroelastic model also shows that in natural hydrogels the US attenuation follows a non-integer frequency law $\nu^{(1+\delta)}$ with $0<\delta\leq 1$ depending on the exponent δ describing the polymer-bounded water viscous interaction.

The experimental measurements confirm the gap between the US speed of propagation in the gel samples and that one of pure water at β close to 1 (100% water). Furthermore, the gel samples with a lower degree of cross-linking (and hence, with higher bounded water volume fraction) show a higher US speed gap at $\beta=1$. The evaluated bounded water fraction ranges from 2% in the PVA samples with six cross-linking cycles to 13% for the PVA samples with two cross-linking cycles.

In the range of experimental conditions ($\beta>0.4$), the bounded water volume fraction ϕ inside each type of PVA hydrogel does not depend on the free water amount. Moreover, as the gel water fraction β is lowered toward zero, the US propagation speed is more and more influenced by the matrix elasticity and increases in samples with higher network cross-linking in agreement with the classical rheological law.

The experimental data also show that the US attenuation in hydrogels decreases with the increase in the water volume fraction β in a linear way in agreement with the theoretical forecast.

All these results have been obtained by introducing into the bi-phasic theory the interaction of the bounded water around the polymer network that is peculiar of hydrogels. As a consequence of that, the proposed bi-phasic model has the capability to describe more appropriately the US propagation both in artificial hydrogels and in soft biological tissues, resulting in a promising tool in the biomedical field either for the development of non-invasive tissue-typing techniques or for the realization of phantoms for experimental tests such as those regarding the thermal therapy.

[1]J. C. Bacri and R. Rajaonarison, "Ultrasonic study of the critical phenomena in gels," J. Phys. (France) Lett. **40**, 15–18 (1979).

[2]J. P. Jarry and G. D. Patterson, "Hypersonic relaxation in polybutadiene and polyisoprene," J. Polym. Sci., Polym. Phys. Ed. **19**, 1791–1797 (1981).

[3]J. C. Bacri, J. M. Courdille, J. Dumas, and R. Rajaonarison, "Ultrasonic waves: A tool for gelation process measurements," J. Phys. (France) Lett. **41**, 369–372 (1980).

[4]K. Yuan, Z. Hu, and Y. Li, "Polymer gel as thermally responsive attenuator for ultrasonic waves," Appl. Phys. Lett. **74**, 2233–2235 (1999).

[5]M. L. Mather and C. Baldock, "Ultrasound tomography imaging of radiation dose distributions in polymer gel dosimeters: Preliminary study," Med. Phys. **30**, 2140–2148 (2003).

[6]F. A. Duck, *Acoustic Properties of Tissue at Ultrasonic Frequencies* (Academic, London, 1990), Chap. 4, pp. 75–99.

[7]F. W. Kremkau, R. W. Barnes, and C. P. McGraw, "Ultrasonic attenuation and propagation speed in normal human brain," J. Acoust. Soc. Am. **70**, 29–38 (1981).

[8]J. W. Wladimiroff, I. L. Craft, and D. G. Talbert, "In vitro measurements of sound velocity in human fetal brain tissue," Ultrasound Med. Biol. **1**, 377–382 (1975).

[9]D. De Rossi, A. Nannini, and C. Domenici, "Artificial sensing skin mimicking mechanoelectrical conversion properties of human dermis," IEEE Trans. Biomed. Eng. **35**, 83–92 (1988).

[10]S. Lochhead, D. Bradwell, R. Chopra, and M. J. Bronskill, "A gel phantom for the calibration of MR-guided ultrasound thermal therapy," in 2004 IEEE Ultrasonics Symposium, Montreal, Canada (2004), Vol. **2**, pp. 1481–1483.

[11]G. Divkovic, M. Liebler, K. Braun, T. Dreyer, P. Huber, and J. Jenne, "Thermal properties and changes of acoustic parameters in an egg white phantom during heating and coagulation by high intensity focused ultrasound," Ultrasound Med. Biol. **33**, 981–986 (2007).

[12]M. Ziol, A. Handra-Luca, A. Kettaneh, C. Christidis, F. Mal, F. Kazemi, V. de Lédinghen, P. Marcellin, D. Dhumeaux, J.-C. Trinchet, and M. Beaugrand, "Noninvasive assessment of liver fibrosis by measurement of stiffness in patient with chronic hepatitis C," Hepatology (Philadelphia, PA, U. S.) **41**, 48–54 (2005).

[13]G. P. Berry, J. C. Bamber, C. G. Armstrong, N. R. Miller, and P. E. Barbonne, "Toward an acoustic model-based poroelasticity imaging method: I. Theoretical foundation," Ultrasound Med. Biol. **32**, 547–567 (2006).

[14]J. Bercoff, M. Tanter, and M. Fink, "Supersonic shear imaging: A new technique for soft tissue elasticity mapping," IEEE Trans. Ultrason. Ferroelectr. Freq. Control **51**, 396–409 (2004).

[15]F. A. Duck, *Acoustic Properties of Tissue at Ultrasonic Frequencies* (Academic, London, 1990), Chap. 4, pp. 112–113.

[16]M. A. Biot, "General theory of three-dimensional consolidation," J. Appl. Phys. **12**, 155–164 (1941).

[17]M. A. Biot, "Theory of propagation of elastic waves in a fluid-saturated porous solid. II. High frequency range," J. Acoust. Soc. Am. **28**, 179–191 (1956).

[18]D. L. Johnson, D. L. Hemmick, and H. Kojima, "Probing porous media with first and second sound. I. Dynamic permeability," J. Appl. Phys. **76**, 104–114 (1994); D. L. Johnson, T. J. Plona, and H. Kojima, "Probing porous media with first and second sound. II. Acoustic properties of water-saturated porous media," *ibid.* **76**, 115–125 (1994).

[19]D. L. Johnson and S. Kostek, "A limitation of the Biot–Gardner theory of extensional waves in fluid-saturated porous cylinders," J. Acoust. Soc. Am. **97**, 741–744 (1995).

[20]E. R. Hughes, T. G. Leighton, G. W. Petley, P. R. White, and R. C. Chivers, "Estimation of critical and viscous frequencies for Biot theory in cancellous bone," Ultrasonics **41**, 365–368 (2003).

[21]D. L. Johnson, "Theory of frequency dependent acoustics in patchy-saturated porous media," J. Acoust. Soc. Am. **110**, 682–694 (2001).

[22]J. Toms, T. M. Muller, R. Ciz, and B. Gurevich, "Comparative review of theoretical models for elastic wave attenuation and dispersion in partially saturated rocks generation," Soil Dyn. Earthquake Eng. **26**, 548–565 (2006).

[23]M. A. Biot, "Theory of propagation of elastic waves in a fluid-saturated porous solid. I. Low-frequency range," J. Acoust. Soc. Am. **28**, 168–178 (1956).

[24]M. A. Biot, "The elastic coefficients of the theory of consolidation," J. Appl. Mech. **24**, 594–601 (1957).

[25]D. L. Johnson, "Elastodynamics of gels," J. Chem. Phys. **77**, 1531–1539 (1982).

[26]R. N. Chandler, "Transient streaming potential measurements on fluid-saturated porous structures: An experimental verification of Biot's slow wave in the quasi-static limit," J. Acoust. Soc. Am. **70**, 116–121 (1981).

[27]A. Peters and S. J. Candau, "Kinetics of swelling of spherical and cylindrical gels," Macromolecules **21**, 2278–2282 (1988).

[28]D. L. Johnson, "Equivalence between fourth sound in liquid He II at low temperature and the Biot slow wave in consolidated porous media," Appl. Phys. Lett. **37**, 1065–1067 (1980).

[29]R. C. Lee, E. H. Frank, A. J. Grodzinsky, and D. K. Royalance, "Oscillatory compressional behavior of articular cartilage and its associated electromechanical properties," J. Biomech. Eng. - Trans. ASME **103**, 280–292 (1981).

[30]P. Chiarelli and D. De Rossi, "Determination of mechanical parameters related to the kinetics of swelling in an electrically activated contractile gel," Prog. Colloid Polym. Sci. **78**, 4–8 (1988).

[31]T. Tanaka and D. J. Fillmore, "Kinetics of swelling of gels," J. Chem. Phys. **70**, 1214–1218 (1979).

[32]P. Chiarelli and D. De Rossi, "Modeling and mechanical characterization of thin fibers of contractile polymer hydrogel," J. Intell. Mater. Syst. Struct. **3**, 396–417 (1992).

[33]P. Chiarelli, C. Domenici, and G. Genuini, "Crazing dynamics in the swelling of thermally cross-linked PVA-PAA films," J. Mater. Sci.: Mater. Med. **4**, 5–11 (1993).

[34]J. G. Berryman, "Confirmation of Biot's theory," Appl. Phys. Lett. **37**, 382–384 (1980).
[35]T. Naganishi, M. Suzuki, and H. Ohigashi, "Ultrasonic transducers," U.S. Patent No. 4,296,349 (20 October 1981).
[36]M. Suzuki and O. Hirasa, "An approach to artificial muscle using polymer gels formed by micro-phase separation," *Advances in Polymer Science* (Springer-Verlag, Berlin, 1993), Vol. **110**. pp. 241–261.
[37]E. A. Zabolotskaya and R. V. Khokhlov, "Quasi-plane waves in nonlinear acoustic of confined beams," Sov. Phys. Acoust. **15**, 35–40 (1969).
[38]V. P. Kuznetsov, "Equation of nonlinear acoustic," Sov. Phys. Acoust. **16**, 467–470 (1970).
[39]X. Yang and R. O. Cleveland, "Time domain simulation of nonlinear acoustic beams generated by rectangular piston with application to harmonic imaging," J. Acoust. Soc. Am. **117**, 113–123 (2005).
[40]S. J. Kowalski, "Ultrasonic waves in diluted and densified suspensions," Ultrasonics **43**, 101–111 (2004).